Journal of Power Sources 203 (2012) 130–134

Contents lists available at SciVerse ScienceDirect

Journal of Power Sources

journal homepage: www.elsevier.com/locate/jpowsour

Short communication

Highly conductive three-dimensional graphene for enhancing the rate performance of $LiFePO_4$ cathode

Yufeng Tang, Fuqiang Huang*, Hui Bi, Zhanqiang Liu, Dongyun Wan

CAS Key Laboratory of Materials for Energy Conversion, Shanghai Institute of Ceramics, Chinese Academy of Sciences, Shanghai 200050, China

ARTICLE INFO

Article history:
Received 26 October 2011
Received in revised form
29 November 2011
Accepted 7 December 2011
Available online 16 December 2011

Keywords:
Graphene
Network
$LiFePO_4$
Electrode materials
Lithium ion battery
High rate

ABSTRACT

In this paper, three-dimensional (3D) graphene network was prepared by chemical vapor deposition (CVD) on 3D porous Ni template. The as-prepared 3D graphene showed high conductivity of ~600 S cm^{-1} and low square resistance of 1.6 Ω sq^{-1}. With the aid of 3D graphene network, the poorly conductive $LiFePO_4$ exhibited high conductivity and good rate performance of 109 mA h g^{-1} at 10 C, indicating potential application in high rate lithium ion batteries.

1. Introduction

Lithium ion batteries with high rate performance have been considered as potential power sources for electric vehicles and high-power devices [1,2]. However, the low electronic and ionic conductivities of the electrode materials limit their practical applications [3–6]. An optimized design of electrode materials for high rate lithium ion batteries should be the introduction of conducting networks through which the mixed conductivity of electrode materials could be improved [7]. Over past years, extensive effort has been made to enhance the mixed conductivity of electrode materials by admixing high conductive carbon-based materials as conducting networks [8–13].

Recently, graphene, a new two-dimensional carbon material, has been treated as potential alternative for common carbon-based conductive phase in lithium ion batteries because of its high electrons mobility, high surface area and chemical tolerance [14–16]. Unfortunately, the graphene synthesized by chemical exfoliation have lots of structure defects and grain boundaries [17,18]. Too many defects and high boundary resistance of graphene might be ineligible at very high charge-discharge current density. Compared with above methods, 3D graphene network prepared by CVD growth on Ni foam exhibits extremely high electrical conductivity and low inter-sheet junction contact resistance [19]. Therefore, this 3D graphene network with high quality and conductivity should be desirable and significant for electrode materials.

As a promising cathode material, $LiFePO_4$ has attracted much attention due to its low cost, low toxicity, and increased safety. However, the major drawback of with $LiFePO_4$ is the low intrinsic electronic conductivity and the poor lithium ions conductivity, which have limited its applications in high power device. In this article, we describe the synthesis of the 3D graphene network and 3D graphene/$LiFePO_4$ composite. The high conductive (~600 S cm^{-1}) 3D graphene, which has few defects and grain boundaries, is expected to give an ideal conducting network for electrode materials. And the 3D graphene/$LiFePO_4$ composite was tested as an anode material for lithium ion battery, presenting high conductivity and good rate performance even at high current density.

2. Experimental

2.1. Preparation of 3D graphene networks

The synthesis of 3D graphene network was performed through a CVD approach. Commercial porous Ni was used as growth template. Before CVD growth, the porous Ni was immersed in a dilute solution of acetic acid for 30 min to remove oxide layer. The clean Ni template was heated to 1000 °C in ~40 min under H_2 (200 sccm).

* Corresponding author at: Shanghai Institute of Ceramics, Chinese Academy of Sciences, Shanghai 200050, China. Tel.: +86 21 52411620; fax: +86 21 52416360.
E-mail address: huangfq@mail.sic.ac.cn (F. Huang).

0378-7753/$ – see front matter © 2011 Elsevier B.V. All rights reserved.
doi:10.1016/j.jpowsour.2011.12.011

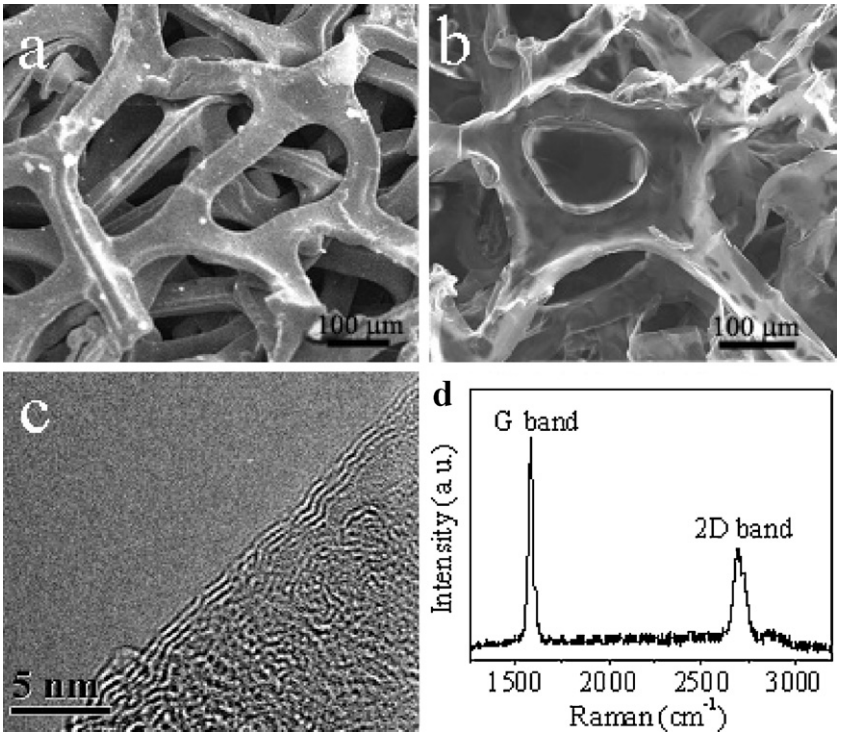

Fig. 1. SEM images of (a) the Ni foam template and (b) 3D graphene network, (c) TEM image of graphene sheet separated from the 3D graphene network, and (d) Raman spectra of 3D graphene network.

After annealing for 40 min, a gas mixture flow of CH_4, H_2 and Ar was introduced to initiate graphene growth for 30 min, and the specific flow rate was 2/50/300 (CH_4/H_2/Ar) in sccm. After growth, the sample was rapidly cooled to 500 °C at a rate of ~200 °C min^{-1} under Ar and H_2. The Ni template covered with graphene was drop-coated with a poly(methyl methacrylate) (PMMA) solution (4% in anisole), and then baked at 100 °C for 2 h. The PMMA/graphene/Ni network was obtained after solidification. Then the samples were put into a 1 M HCl solution at 60 °C to completely dissolve the Ni template. Finally 3D graphene network was obtained after removing PMMA in acetone.

2.2. Preparation of $LiFePO_4$

$LiFePO_4$ was synthesized by solid-state reaction. The starting materials (LiH_2PO_4, $FeC_2O_4{\cdot}2H_2O$ and sucrose) were mixed by ball-milling for 12 h using zirconia milling media, in ethanol. After drying, the precursor was heated at 350 °C for 4 h in flowing Ar. Final calcination for crystallization of the olivine phase was done at 800 °C for 10 h in an H_2–Ar (5:95) atmosphere. The carbon content of $LiFePO_4$ is 2 wt%.

2.3. Preparation of 3D graphene/$LiFePO_4$

The fabrication progress of 3D graphene/$LiFePO_4$ composite was as follows: 3D graphene was added to the *N*-methyl pyrrolidinone (NMP) suspension of as-prepared $LiFePO_4$ with $LiFePO_4$:graphene = 95:5 (wt). After stirring smoothly for 0.5 h, NMP was evaporated at 80 °C, and the 3D graphene/$LiFePO_4$ composite was obtained.

The structure and morphology of the products were characterized by Scanning Electron Microscope (SEM, JEOL JSM-6510). TEM images were performed on a JEOL JEM 2100F transmission electron microscope with an accelerating voltage of 200 kV. The GSs were characterized with Raman spectroscopy having laser excitation energy of 514 nm in Renishaw inVia Reflex laser Raman. To evaluate the conductivity of 3D graphene, current–voltage characteristics of 3D graphene film were carried out with CHI660C electrochemical workstation.

The charge and discharge capacities were measured with coin cells in which a lithium metal foil was used as the counter electrode. The electrolyte employed was 1 M solution of $LiPF_6$ in ethylene carbonate and dimethyl carbonate (EC + DMC) (1:1 in volume). The active materials powder (85 wt%), acetylene black (5 wt%) and polyvinylidene fluoride (PVDF) binder (10 wt%) were homogeneously mixed in NMP solvent with magnetic stirring. After stirring for 3.5 h, the slurry was coated uniformly on an aluminum foil. Finally, the electrode was dried under vacuum at 110 °C for 10 h. Cell assembly was carried out in an argon-filled glove box (German, M. Braun Co., $[O_2] < 1$ ppm, $[H_2O] < 1$ ppm). The coin cells were cycled under different current densities between cutoff voltages of 4.2 and 2.5 V on a CT2001A cell test instrument (LAND Electronic Co.) at room temperature.

3. Result and discussion

Fig. 1 shows representative SEM images of Ni template and as-prepared 3D graphene network. From Fig. 1a, it can be found that the Ni template has a 3D porous structure with porous diameter of 50–100 μm. After 10 min CVD growth in CH_4/H_2/Ar atmosphere, the entire Ni surface was fully covered by graphene. The interconnected 3D graphene network is obtained after acid etching of the Ni skeleton, as shown in Fig. 1b. It is interesting that the 3D graphene network is made up of hollow graphene tubes of about 20 μm in diameter. The graphene tubes are unclosed, and lots of porous can be found in the wall of the tubes. This 3D graphene has a high specific surface area (500–600 m^2 g^{-1}), which is dependent on the porosity and density of the Ni template. The TEM image in Fig. 1c presents one of the separated graphene sheets from 3D network. It is clear that the graphene sheet has three layers with the thickness of ~2 nm.

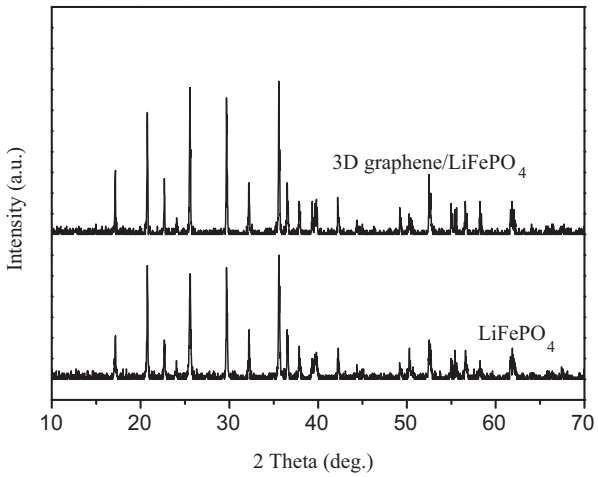

Fig. 2. XRD patterns of 3D graphene/$LiFePO_4$ composite and $LiFePO_4$ without graphene prepared by solid-state reaction.

The layer number of the graphene sheet can be further confirmed by Raman spectra, as shown in Fig. 1d, wherein only G-band ($\sim$1580 cm^{-1}) and 2D-band ($\sim$2700 cm^{-1}) are observed. The G-band corresponds to the E_{2g} phonon at the Brillouin zone center, whereas the 2D-band relates to the second order of zone boundary phonons [20]. The 2D-band peak position of $\sim$2700 cm^{-1} and the intensity ratio of 2D-band to G-band (I_{2D}/I_G) of around 0.47 represent about three graphene layers [21], which is consistent with the result of TEM analysis. It can be found that no D-band in the 3D graphene sample is observed in Fig. 1d, suggesting high graphene quality. Electrical analysis shows that the 3D graphene has high electrical conductivities of $\sim$600 S cm^{-1} and low square resistance of 1.6 Ω sq^{-1}, better than the graphene from chemical exfoliation [22]. Thus, the 3D graphene network can provide fast electrons transport channels for electrode materials, promising good rate performance at high charge–discharge current density.

As $LiFePO_4$ has poor electronic and ionic conductivities, the development of high conductive $LiFePO_4$ is essential for their practical application in lithium ion batteries. The 3D graphene/$LiFePO_4$ composites have been prepared by combining 3D graphene with $LiFePO_4$. Fig. 2 shows the XRD patterns of 3D graphene/$LiFePO_4$ and $LiFePO_4$ without 3D graphene. The two patterns both show well-resolved diffraction peaks indexed to olivine $LiFePO_4$ (JCPDS No. 81-1173). This demonstrates that well-crystallized $LiFePO_4$ is obtained by solid-state reaction. There is no obvious diffraction peak of graphene at $\sim$25° [23], which might be due to its low content in the graphene/$LiFePO_4$ sample.

The general morphology of $LiFePO_4$, graphene/$LiFePO_4$ composite and the electrode surface is shown in Fig. 3. Fig. 3a shows the SEM image of the $LiFePO_4$, which has a well-dispersed structure, although a few agglomerations exist. The typical size of the $LiFePO_4$ particles (Fig. 3b) is in the range 0.5–1.0 μm. It can be seen from Fig. 3c that the graphene/$LiFePO_4$ composite has similar porous network to 3D graphene. The outer and the inner of graphene tubes are both coated by $LiFePO_4$ particles. Fig. 3d shows the surface morphology of 3D graphene/$LiFePO_4$ composite electrode. Although the 3D graphene network is broken in somewhere during the preparation of 3D graphene/$LiFePO_4$ electrode, it still maintains interconnected network. The continuous graphene can provide a high conductive network for $LiFePO_4$ electrode.

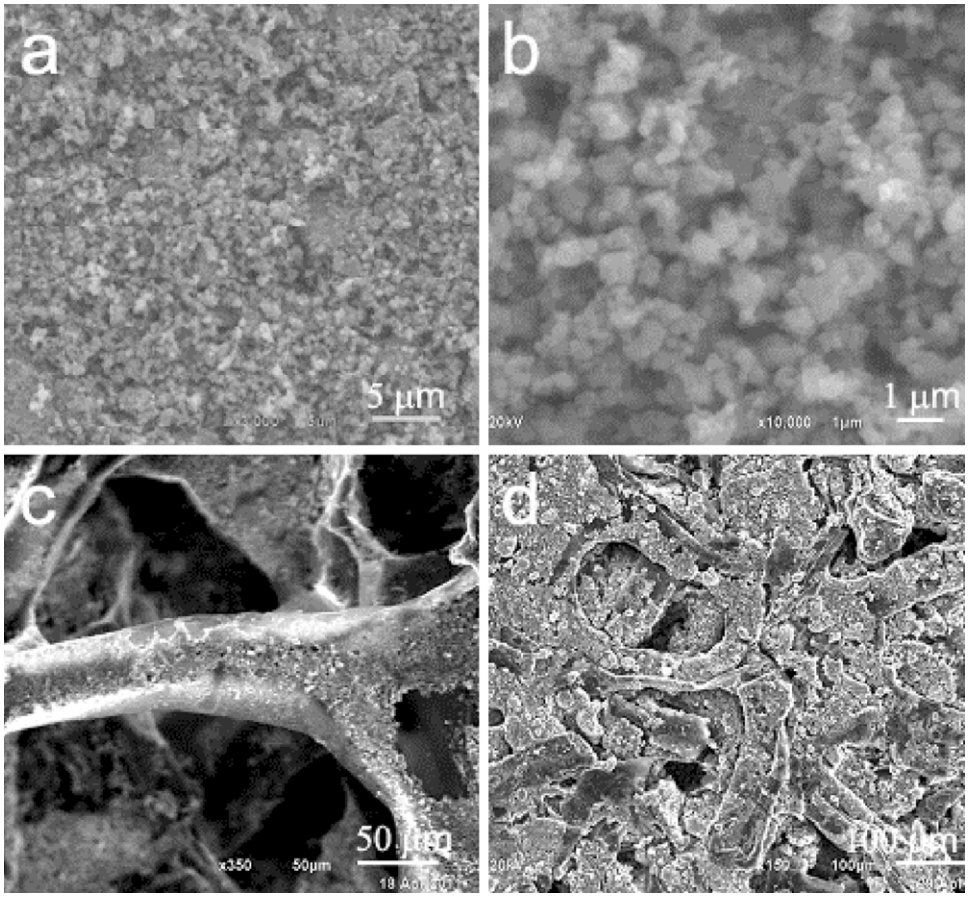

Fig. 3. SEM images of (a, b) the as-prepared $LiFePO_4$, (c) 3D graphene/$LiFePO_4$ composite and (d) the electrode surface of 3D graphene/$LiFePO_4$.

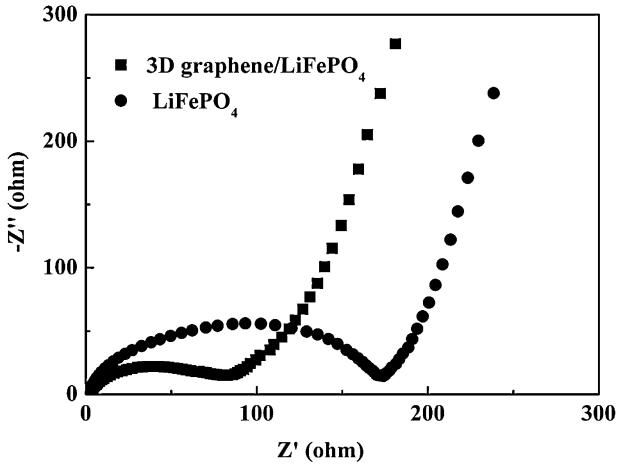

Fig. 4. Complex impedance plots at room temperature for 3D graphene/$LiFePO_4$ composite and $LiFePO_4$.

In order to evaluate the conductivity of 3D graphene/$LiFePO_4$, the AC impedance spectroscopes at ambient temperature were performed. As shown in Fig. 4, the total impedance of $LiFePO_4$ without graphene is 170 Ω higher than ~90 Ω of 3D graphene/$LiFePO_4$. The total impedance of each sample, which is mainly induced by the charge transfer between the electrolyte and the electrode interface, can be obtained from the intersection of the semicircle with the real axis at the lower frequency side. Since the high conductive 3D graphene network is favorable to fast transport of electrons, the increase of the conductivity in the 3D graphene/$LiFePO_4$ is mainly due to the increase of the electronic conductivity.

The electrochemical property of the 3D graphene/$LiFePO_4$ composite was investigated by charge–discharge cycle analysis. The cell was first cycled at 0.2 C for 5 cycles, and then the discharge–charge rate was increased stepwise to as high as 10 C. It can be seen in Fig. 5a that the 3D graphene/$LiFePO_4$ can sustain excellent charge and discharge rates. The cell voltage decreases with the increasing current density. It is 3.38 V at 0.2 C and drops to about 3.15 V at 10 C. Moreover, the charge capacity and the discharge capacity exhibit a tendency to decrease with increasing discharge current density.

Fig. 5b compares the rate performance of 3D graphene/$LiFePO_4$ composite with pure $LiFePO_4$. Although the two samples have comparable capacity at low rate, the performance of $LiFePO_4$ without graphene becomes worse at high rate above 1 C. For 3D graphene/$LiFePO_4$, a specific discharge capacity of around 158 mA h g^{-1} is obtained at a rate of 0.2 C; this value is lowered to 150, 144, and 135 mA h g^{-1} at 1, 2, and 5 C, respectively. Even at the rate of 10 C, the specific discharge capacity is still 109 mA h g^{-1}. Cells discharged to 69% of their initial capacity at a rate of 10 C, while $LiFePO_4$ without graphene only to 26% at the same discharge rate. The rate performance of 3D graphene/$LiFePO_4$ is not only better than $LiFePO_4$ without 3D graphene, but also better than the samples prepared by solid methods in previous reports [24,25]. The rate performance of 3D graphene/$LiFePO_4$ can be further improved though in-situ growth of nanosized $LiFePO_4$ on the surface of 3D graphene, which will be reported in the following work. The reversibility of 3D graphene/$LiFePO_4$ is demonstrated by the fact that the capacity of 153 mA h g^{-1} is reached again once the rate is returned to 0.2 C. Above results indicate that the 3D graphene network provides the possibility of fast transport of electrons cathode, which is favorable for $LiFePO_4$ to maintain high capacity even at high charge–discharge rate.

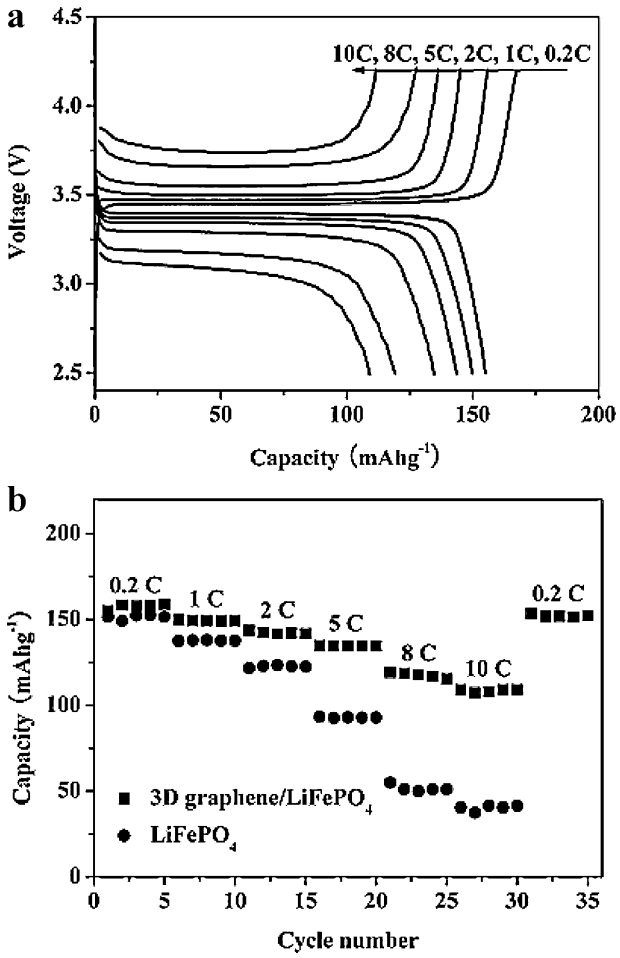

Fig. 5. (a) The first charge–discharge curves for 3D graphene/$LiFePO_4$ composite between 2.5 and 4.2 V at different current densities. (b) Rate performance of $LiFePO_4$ and 3D graphene/$LiFePO_4$ composite.

4. Conclusions

In summary, the 3D graphene was prepared by CVD method and used as conducting network to improve the rate performance of electrode materials. The 3D graphene possesses high conductivity of 600 S cm^{-1} and low square resistance of 1.6 Ω sq^{-1}. And electrochemical performance measurements have indicated that the 3D graphene/$LiFePO_4$ composite exhibits high reversible capacity and good rate performance, implying potential application in high rate lithium ion batteries.

Acknowledgments

This work is financially supported by National 973 & 863 Program of China Grant Nos. 2009CB939903 & 2011AA050505, NSF of China Grant Nos. 50821004, 61106088, 50902143, 21101164, 61076062 & 51102263, National Science Foundation of China Grant 20901083 and Science and Technology Commission of Shanghai Grant Nos. 10520706700 & 10JC1415800.

References

[1] K. Kang, Y.S. Meng, J. Breger, C.P. Grey, G. Ceder, Science 311 (2006) 977.
[2] J. Maier, Nat. Mater. 4 (2005) 805.
[3] Y.S. Hu, Y.G. Guo, R. Dominko, M. Gaberscek, J. Jamnik, J. Maier, Adv. Mater. 19 (2007) 1963.
[4] S.Y. Chung, J.T. Bloking, Y.M. Chiang, Nat. Mater. 1 (2002) 123.
[5] A. Yamada, H. Koizumi, S.I. Nishimura, N. Sonoyama, R. Kanno, M. Yonemura, T. Nakamura, Y. Kobayashi, Nat. Mater. 5 (2006) 357.

[6] R. Amin, P. Balaya, J. Maier, Electrochem. Solid-State Lett. 10 (2007) A13.
[7] W.M. Chen, L. Qie, L.X. Yuan, S.A. Xia, X.L. Hu, W.X. Zhang, Y.H. Huang, Electrochim. Acta 56 (2011) 2689.
[8] Z. Liu, S.W. Tay, L. Hong, J.Y. Lee, J. Solid State Electrochem. 15 (2011) 205.
[9] Z.H. Chen, J.R. Dahn, J. Electrochem. Soc. 149 (2002) A1184.
[10] Y. Zhou, J. Wang, Y. Hu, R. O'Hayreb, Z. Shao, Chem. Commun. 46 (2010) 7151.
[11] R. Dominko, M. Bele, J.M. Goupil, M. Gaberscek, D. Hanzel, I. Arcon, J. Jamnik, Chem. Mater. 19 (2007) 2960.
[12] Y.G. Wang, Y.R. Wang, E.J. Hosono, K.X. Wang, H.S. Zhou, Angew. Chem. Int. Ed. 47 (2008) 7461.
[13] H.M. Yu, X.B. Teng, J. Xie, G.S. Cao, X.B. Zhao, Electrochem. Solid-State Lett. 14 (2011) A19.
[14] L. Shen, C. Yuan, H. Luo, X. Zhang, S. Yang, X. Lu, Nanoscale 3 (2011) 572.
[15] K. Chang, W. Chen, Chem. Commun. 47 (2011) 4252.
[16] Y. Ding, Y. Jiang, F. Xu, J. Yin, H. Ren, Q. Zhuo, Z. Long, P. Zhang, Electrochem. Commun. 12 (2010) 10.
[17] A.B. Kaiser, C. Gómez-Navarro, R.S. Sundaram, M. Burghard, K. Kern, Nano Lett. 9 (2009) 1787.
[18] I.N. Kholmanov, J. Edgeworth, E. Cavaliere, L. Gavioli, C. Magnuson, R.S. Ruoff, Adv. Mater. 23 (2011) 1675.
[19] Z. Chen, W. Ren, L. Gao, B. Liu, S. Pei, H. Cheng, Nat. Mater. 10 (2011) 424.
[20] Z. Luo, T. Yu, J. Shang, Y. Wang, S. Lim, L. Liu, G.G. Gurzadyan, Z. Shen, J. Lin, Adv. Funct. Mater. 21 (2011) 911.
[21] R. Wang, Y. Hao, Z. Wang, H. Gong, J.T.L. Thong, Nano Lett. 10 (2010) 4844.
[22] W. Gao, L.B. Alemany, L. Ci, P.M. Ajayan, Nat. Chem. 1 (2009) 403.
[23] S. Ding, J.S. Chen, D. Luan, F.Y.C. Boey, S. Madhavi, X.W. Lou, Chem. Commun. 47 (2011) 5780.
[24] S.Y. Chung, J.T. Blokng, Y.M. Chiang, Nat. Mater. 1 (2002) 123.
[25] N. Ravet, Y. Chouinard, J.F. Magnan, S. Besner, M. Gauthier, M. Armand, J. Power Sources 97–98 (2001) 503.